HHS Public Access

Author manuscript

Biofabrication. Author manuscript; available in PMC 2020 July 10.

Published in final edited form as:

Biofabrication. ; 11(4): 045009. doi:10.1088/1758-5090/ab2b4d.

3D printed coaxial nozzles for the extrusion of hydrogel tubes toward modeling vascular endothelium

S. Cem Millik[1], **Ashley M. Dostie**[1], **Dylan G. Karis**[1], **Patrick T. Smith**[1], **Michael McKenna**[2], **Nathan Chan**[3], **Chad D. Curtis**[2], **Elizabeth Nance**[2,3], **Ashleigh B. Theberge**[1,4], **Alshakim Nelson**[1]

[1]Department of Chemistry, University of Washington, Seattle, WA, USA

[2]Department of Chemical Engineering, University of Washington, Seattle, WA, USA

[3]Molecular Engineering and Sciences Institute, University of Washington, Seattle, WA, USA

[4]Department of Urology, University of Washington School of Medicine, Seattle, WA, USA

Abstract

Engineered tubular constructs made from soft biomaterials are employed in a myriad of applications in biomedical science. Potential uses of these constructs range from vascular grafts to conduits for enabling perfusion of engineered tissues and organs. The fabrication of standalone tubes or complex perfusable constructs from biofunctional materials, including hydrogels, via rapid and readily accessible routes is desirable. Here we report a methodology in which customized coaxial nozzles are 3D printed using commercially available stereolithography (SLA) 3D printers. These nozzles can be used for the fabrication of hydrogel tubes via coextrusion of two shear-thinning hydrogels: an unmodified Pluronic® F-127 (F127) hydrogel and an F127-bisurethane methacrylate (F127-BUM) hydrogel. We demonstrate that different nozzle geometries can be modeled via computer-aided design and 3D printed in order to generate tubes or coaxial filaments with different cross-sectional geometries. We were able to fabricate tubes with luminal diameters or wall thicknesses as small as ~150 μm. Finally, we show that these tubes can be functionalized with collagen I to enable cell adhesion, and human umbilical vein endothelial cells can be cultured on the luminal surfaces of these tubes to yield tubular endothelial monolayers. Our approach could enable the rapid fabrication of biofunctional hydrogel conduits which can ultimately be utilized for engineering *in vitro* models of tubular biological structures.

Keywords

3D printing; hydrogel; tubular conduit; endothelial; endothelium; vascular; blood vessel; vasculature

alshakim@uw.edu, abt1@uw.edu.

1. Introduction

Tubular structures are abundant in nature where they function broadly as conduits for the bulk transport of fluids. Examples include the airways and blood vessels of vertebrates, and the xylems and phloems of vascular plants [1, 2]. Fabrication of perfusable structures using biofunctional materials and compatible manufacturing processes is of great interest in the areas of bioengineering (e.g. for *in vitro* assays) and regenerative medicine [3–13]. While tubes are geometrically simple, their fabrication from soft materials is an existing challenge in the field. Common strategies involve casting or rolling a synthetic or natural polymeric material around a mandrel, wherein the diameter of the mandrel determines the tube's luminal diameter. These mandrel-based approaches have generally yielded tubes with properties comparable to those of human blood vessels, however, the utility of these approaches is limited when it comes to the fabrication of tubes with small luminal diameters (<0.5 mm) and arbitrary lengths (>15 cm) [14–20].

An alternative approach for fabricating tubular structures involves material extrusion through dies with annular orifices. Extrusion-based processes are good candidates for this task because they have the ability to produce constructs with complex cross-sectional profiles and hollow internal geometries which are difficult to create using most other types of manufacturing processes [8–10, 12, 13, 21–23].

Standalone tubular structures have been investigated as vascular grafts [19, 20, 24], nerve guidance conduits [18, 25, 26], grafts for urethroplasty [27–29], and tracheal grafts [30]. More complex, perfusable, cell-laden constructs which utilize tubes as a basic structural motif have also been designed to recapitulate tissue or organ function [31–33].

Hydrogels are attractive materials for many biomedical applications due to their significant water content and mechanics reminiscent of soft tissues [34, 35]. However, it remains challenging to reconcile biocompatibility, bioactivity, and mechanics in hydrogels with processability in the context of extrusion [36]. Previous reports have succeeded in outlining sets of biochemical and biophysical material properties which are essential for the recapitulation of many physiological functions [37–39], yet the incorporation of these properties into materials used in extrusion-based fabrication processes remains a challenge.

Hydrogels that have thus far been processed into tubular structures for potential biomedical applications include those based on gelatin [8, 9], hyaluronic acid [10], alginate [12, 13], collagen [14, 16], poly(vinyl alcohol) [17, 20], silk fibroin [18], fibrin [19], and decellularized extracellular matrix [21]. Recently, Pi *et al* [8] have demonstrated coaxial extrusion-based fabrication of circumferentially layered tissue-engineered tubular constructs using materials based on methacrylated gelatin, alginate, and acrylated multi-arm poly(ethylene glycol). The authors produced these constructs using urothelial cells, vascular endothelial cells, and smooth muscle cells. These tissue-engineered constructs represent an important step toward creating engineered replacements for tubular biological structures. However, this platform involves handmade nozzles, which may restrict the platform's accesibility and customizability. Here we report a practical and versatile 3D printing-enabled platform for the extrusion-based fabrication of tubular hydrogel constructs and multi-

material coaxial filaments (figure 1). Additionally, we demonstrate the fabrication of bioactive collagen-functionalized hydrogel tubes for the culture of human umbilical vein endothelial cells (HUVECS).

Our platform utilizes 3D printed and fully customizable coaxial nozzles in combination with extrudable hydrogels based on a derivative of Pluronic® F-127. The employment of 3D printing in our work highlights the utility of additive manufacturing in the rapid design, fabrication, and iteration of extrusion hardware posessing relatively complex geometries. The platform outlined here, including the materials and process-design principles highlighted, can broadly serve as an example of effective implementation of design for additive manufacturing in the context of biofabrication. Finally, a notable advantage of this platform stems from its accessibility to other laboratories. The computer-aided design (CAD) files of the coaxial nozzles (available in the supplementary material online at stacks.iop.org/BF/11/045009/mmedia) can be modified to meet a variety of needs, and the nozzles can be printed on commercially available desktop SLA 3D printers.

2. Materials and methods

2.1 Materials

Pluronic® F-127 (P2443–1KG; referred to as F127), phenol red solution (P0290–100ML; 0.5%), sodium hydroxide solution (S2770–100ML; 1.0 M), 2-hydroxy-4’-(2-hydroxyethoxy)-2-methylpropiophenone (410896–10 G; 98%; referred to as Irgacure 2959), and 2-acrylamido-2-methyl-1-propanesulfonic acid sodium salt solution (655821–250 ML; 50 wt%; referred to as AMPS) were all purchased from Sigma Aldrich. Dibutyltin dilaurate (D0303; >95.0%) was purchased from TCI America. 2-Isocyanatoethyl methacrylate (ACT34296) was purchased from Arctom Chemicals. $CDCl_3$ (DLM-7-PK; 99.8%) was purchased from Cambridge Isotope Laboratories. Common solvents (Certified ACS) and phosphate-buffered saline (PBS) tablets (BP2944100) were purchased from Fisher Scientific. Collagen I from rat tail tendon (354249; 8.3 mg ml^{-1} in 0.02 M acetic acid) was purchased from Corning. Ammonium hydroxide (AX1303; 28.0–30.0 wt%) was purchased from EMD Millipore. Autodesk Standard Clear Prototyping Resin (also known as PR48) was purchased from Colorado Photopolymer Solutions. Formlabs Clear photopolymer resin (FLGPCL04) was purchased from Formlabs.

HUVECs (C2517A; single donor; in EGM-2; referred to as HUVECs) and endothelial cell growth medium (CC-3162; referred to as EGM-2) were purchased from Lonza. Penicillin-streptomycin cocktail (15140122; 10000 U ml^{-1}), ethidium homodimer-1 (E1169), calcein AM (C3100MP), and 4’,6-diamidino-2-phenylindole (D1306; referred to as DAPI) were all purchased from Thermo Fisher Scientific. Subculture Reagent Kit (090 K; containing HBSS, Trypsin/EDTA & Trypsin Neutralizing Solution) was purchased from Cell Applications. Paraformaldehyde solution (50–980-487; 16%), bovine serum albumin (BP9706100; referred to as BSA), polysorbate 80 (AC278632500; referred to as P80), and Alexa Fluor 488-goat anti-mouse IgG (NC0675427; IgG polyclonal; H+L) were all purchased from Fisher Scientific. Triton X-100 (X100–100ML) was purchased from Sigma Aldrich. Mouse anti-human CD31 (MCA1738; IgG1 monoclonal; clone WM59) was purchased from Bio-Rad Laboratories. All reagents were used as received unless otherwise specified.

2.2 Instrumentation

The $_1$H NMR spectrum was obtained using a Bruker AVANCE series instrument with 500 MHz frequency. Gel permeation chromatography was performed using a Waters Breeze 2 chromatograph equipped with two 10 μm Malvern columns (300 mm × 7.8 mm) connected in series with increasing pore size (1000, 10 000 Å), using chloroform as the eluent, and calibrated with poly(ethylene glycol) standards (102–40 000 g mol^{-1}). Rheometric experiments were performed using a TA Instruments Discovery Hybrid Rheometer-2 equipped with an Advanced Peltier Plate system for temperature control, and a 365 nm LED UV-curing accessory with disposable acrylic plates for photorheology experiments. All rheometric experiments were performed using a stainless steel 20 mm upper plate. Coaxial nozzles were 3D printed using an Autodesk Ember DLP 3D Printer or a Formlabs Form 2 SLA 3D Printer. Fluorescence microscopy was performed on a Zeiss Axiovert 200 with Axiocam 503 mono camera. Confocal microscopy was performed on a custom-built simultaneous 4-channel Nikon AR1 with cMOS camera with *xyz*-motorization.

2.3 Synthesis of F127-BUM

The synthesis of F127-bisurethane methacrylate (F127-BUM) is described in full detail in the supplementary material. Briefly, F127 (60 g, 4.8 mmol) was dried under vacuum, and anhydrous CH_2Cl_2 (550 ml) was charged to the flask. The mixture was stirred until complete dissolution of the F127 was observed. Dibutyltin dilaurate was then added, and the 2-isocyanatoethyl methacrylate (3.5 ml, 24.8 mmol) was diluted in anhydrous CH_2Cl_2 (50 ml) and added dropwise to the reaction mixture. The reaction was allowed to proceed for 2 d before being quenched by the addition of MeOH. The F127-BUM was precipitated in Et_2O before separation via centrifugation. The F127-BUM precipitate was finally washed in Et_2O, prior to being dried under vacuum.

2.4 Preparation of F127-based hydrogels

2.4.1 Preparation of F127-BUM hydrogel with collagen I additive—

Collagen I (1.2 ml; 8.3 mg ml^{-1} in 0.02 M acetic acid) was added to chilled, sterilized dH_2O (2.21 ml). The mixture was swirled thoroughly before the addition of F127-BUM (1.5 g). Immediately after addition of the F127-BUM, the mixture was vortex-mixed and placed on ice for approximately 3 h until dissolution of the F127-BUM was observed. A 5 wt% solution of Irgacure 2959 was prepared by adding sterilized dH_2O to Irgacure 2959 and incubating for 30 min at 70 °C before briefly vortex-mixing. After dissolution of the F127-BUM, the Irgacure 2959 solution (100 μl; 5 wt%) was added to the gel, and the gel was vortex-mixed again briefly. The gel was kept on ice overnight and vortex-mixed the following day, followed by centrifugation at approximately 600 g for 1 min This process was repeated two or three times until a homogeneous, slightly turbid gel was observed. The gel was kept on ice whenever possible during this time. The gel was stored in the dark at 4 °C and used within 3 d. Prior to use, bubbles (if remaining) were eliminated by brief centrifugation at approximately 600 g.

2.4.2 Preparation of F127-BUM hydrogel with AMPS additive—

AMPS solution (1.0 g; 50 wt%) was added to chilled, sterilized dH_2O (2.4 ml). The mixture was swirled

briefly before the addition of F127-BUM (1.5 g). Immediately after addition of the F127-BUM, the mixture was vortex-mixed and placed on ice for approximately 3 h until dissolution of the F127-BUM was observed. Irgacure 2959 solution (100 μl; 5 wt%) was then added to the gel, and the gel was vortex-mixed again briefly. The 5 wt% solution of Irgacure 2959 was prepared as described previously. The gel was also stored and conditioned as described previously.

2.4.3 Preparation of F127-BUM hydrogel without additive—F127-BUM (1.5 g) was added to chilled, sterilized dH_2O (3.4 ml). Immediately after addition of the F127-BUM, the mixture was vortex-mixed and placed on ice for approximately 3 h until dissolution of the F127-BUM was observed. Irgacure 2959 solution (100 μl; 5 wt%) was then added to the gel, and the gel was vortex-mixed again briefly. The 5 wt% solution of Irgacure 2959 was prepared as described previously. The gel was also stored and conditioned as described previously.

2.4.4 Preparation of sacrificial F127 core hydrogel—Unfunctionalized F127 (1.5 g) was added to chilled, sterilized dH_2O (3.5 ml). Immediately after addition of the F127, the mixture was vortex-mixed and phenol red solution (150 μl; 0.5 wt%) was added. NaOH (10 μl; 1.0 M) was also added to bring the gel to approximately pH 7.4. The gel was vortex-mixed again briefly and placed on ice for approximately 3 h until dissolution of the F127 was observed. The gel was stored and conditioned as described previously.

2.5 Coaxial nozzle fabrication

The nozzles were printed using an Autodesk Ember DLP 3D Printer with the Autodesk Standard Clear Prototyping Resin, also known as PR48 (Colorado Photopolymer Solutions) or a Formlabs Form 2 SLA 3D Printer with Formlabs Clear photopolymer resin (Formlabs). In all cases, 50 μm was selected as the layer height. The standoff from the build surface was set to 0 mm, and nozzles were printed such that their superior surfaces made contact with the build surface. Support structures were not used. Following completion of prints, nozzles were rinsed with isopropanol. The nozzles were then purged and dried with pressurized air and post-cured according to the manufacturer's instructions. Following 3D printing and completion of the post-printing steps described, 14 gauge × 0.5 in straight and bent (45°) blunt-tip needles (OK International) were affixed to the superior and lateral inlets, respectively, of each coaxial nozzle. The straight needle was ground short and deburred such that the remaining length of the canula was roughly 5 mm. This measure was taken to reduce the overall height of the fully assembled coaxial nozzle and is not a necessary step. Alternatively, 14 gauge × 0.25 in needles could be used. Loctite 495 cyanoacrylate adhesive was used to affix the needles. Following assembly, each nozzle was washed with 70% isopropanol and stored at room temperature in dH_2O until further use. Prior to use, nozzles were rinsed briefly with 70% EtOH.

2.6 Fabrication of hydrogel tubes

Unless otherwise specified, tubes were fabricated using the largest-size (2 mm outer conduit diameter) nozzle. Gels chilled on ice were loaded into syringes (Nordson EFD), and once the gels reached room temperature, the extrusion set up (figure S7b) was assembled. The

syringe containing the sacrificial (core) gel was affixed to the superior inlet and the syringe containing the outer (shell) gel was affixed to the lateral inlet of the coaxial nozzle (figure 1(b; i)). Syringe barrel adapters (Nordson EFD) were then attached to each syringe. Pressure to drive the syringe pistons was supplied by an in-house N_2 line. The pressure was controlled independently for each syringe around 55–100 kPa, nominally, by 0–210 kPa pressure regulators and gauges. To adjust pressures prior to extrusion, the tubing of each syringe barrel adapter was clamped using a pinch-clamp, and the regulators were set to the desired pressures. To begin extrusion, the tubing of each adapter was unclamped, and after waiting a moment for the coaxial extrusion rate to stabilize, a 4 in × 6 in glass sheet was manually translated under the nozzle to catch the coaxial gel filament. The shell of the coaxial filament (outer gel) was then photo cross-linked for 20 min under a UV lamp (365 nm, 3.3 mW cm^{-2}). The sacrificial core of the coaxial filament (inner gel) was removed via dissolution in aqueous medium to yield the hydrogel tube. 1X PBS was used as the dissolution medium for hydrogel tubes used in cell seeding experiments; dH_2O was used for hydrogel tubes for all other purposes.

2.7 Cell seeding experiments

Overview: The F127-BUM hydrogel with collagen I additive was used in the fabrication of tubes and discs for cell seeding experiments (all parts of figure 3 except figure 3(a; i)). The F127-BUM hydrogel without collagen I additive was used in the fabrication of discs as a negative control (figure 3(a; i)). HUVECs were maintained in endothelial cell growth medium (EGM-2 supplemented with 100 units ml^{-1} penicillin and 100 μg ml^{-1} streptomycin). Cells were maintained in a 37 °C incubator with 5% CO_2. Cells of passage number 4–8 were used for all cell seeding experiments.

2.7.1 Preparation of hydrogel tubes for cell seeding—Preparation of hydrogel tubes for cell seeding is described in detail in the supplementary material. Briefly, following coaxial extrusion and photo-cross-linking as described previously (with the F127-BUM hydrogel with collagen I additive used as the shell), the coaxial filament was placed in 1X PBS and incubated at 37 °C for 1 h to facilitate dissolution of the sacrificial core hydrogel. The resulting tube was sectioned (~20 mm long sections), and the tube sections were sequentially washed with dH_2O, 70% EtOH, and sterilized 1X PBS. The tube sections were then dehydrated in an incubator at 37 °C. Following dehydration, tube sections were submerged in collagen solution (6.0 mg ml^{-1} in 0.014 M acetic acid) and were allowed to rehydrate. Following rehydration, tube sections were briefly exposed to ammonia vapor to facilitate pH- and temperature-dependent cross-linking of the collagen (discussed further in supplementary material). Tube sections were then once again placed in a 37 °C incubator to dehydrate. The rehydration procedure was repeated once more, and following another dehydration, a similar rehydration procedure was carried out with endothelial cell growth medium instead of collagen solution. Following a final dehydration, tube sections were rehydrated with the growth medium and stored in medium at 4 °C until cell seeding.

2.7.2 Fabrication of hydrogel discs and preparation for cell seeding experiments—Fabrication of hydrogel discs and preparation for cell seeding is described in detail in the supplementary material. Briefly, a pair of cured hydrogel sheets were

prepared from F127-BUM hydrogels with and without collagen I additive. The sheets were placed in 1X PBS and incubated at 37 °C for 1 h. A biopsy punch (5 mm) was then used to punch gel discs from the sheets. Discs were sequentially washed with dH_2O, 70% EtOH, and sterilized 1X PBS. Discs made from F172-BUM hydrogel with collagen I additive were dehydrated in an incubator at 37 °C. The discs without collagen (negative control) were transferred to endothelial cell growth medium and stored at 4 °C in medium until cell seeding. Following dehydration, F127-BUM discs with collagen I were subjected to a dehydration/rehydration procedure as described in section 2.7.1: discs were submerged in collagen I solution and were allowed to rehydrate. Following rehydration, discs were briefly exposed to ammonia vapor. Discs were then once again placed in a 37 °C incubator to dehydrate. The rehydration procedure was repeated once more, and following another dehydration, a similar rehydration procedure was carried out with endothelial cell growth medium instead of collagen solution. Following a final dehydration, discs were rehydrated with the growth medium and stored in medium at 4 °C until cell seeding.

2.7.3 HUVEC seeding and culture in tube sections—For cell seeding in tube sections, HUVECs were trypsinized and resuspended at a concentration of approximately $1.0 \times 10_6$ cells ml^{-1} in EGM-2 with penicillin-streptomycin. Sterilized blunt-tip needles (14 gauge × 0.5 in) were attached to 1 ml syringes, and a tube section was gently slipped onto each needle. Tube sections were briefly rinsed by drawing growth medium into, and through, the lumens. Approximately 100 μl of the cell suspension was then drawn through the tube sections so that lumens were filled with cell suspension. Tube sections with syringes attached were transferred to a poly(styrene) BioAssay dish lined with Kimwipes soaked in 1X PBS. The tube sections and syringes were kept horizontally in the BioAssay dish during a 1 h incubation at 37 °C and 5% CO_2. Throughout the incubation, tube sections and attached syringes were rotated 90° every 15 min to ensure uniform access of cells to luminal walls. While in the dish, syringes were kept from rolling using 3D printed poly(lactic acid) syringe stands (FlashForge Creator Pro) (figure S9b). Following the 1 h incubation, tube sections were removed from syringes and transferred to growth medium in a 6-well poly(styrene) culture plate (2 ml of medium per tube section; two tube sections per well) and additionally incubated for up to 72 h at 37 °C and 5% CO_2. Medium was replaced after 48 h in culture. Prior to visualization of cell morphology in tube sections via DAPI staining and indirect immunofluorescence, tube sections were removed from the medium, transferred to a new culture plate, and briefly rinsed with 1X PBS. Cells were fixed at room temperature in 4% paraformaldehyde for 20 min. For rinses and fixation, a 1 ml syringe with a blunt-tip needle was briefly used to draw solution into the lumen of each tube section; each tube section was then immediately slipped off of the syringe needle and into a well of a 6-well poly(styrene) culture plate containing enough solution to submerge the tube section.

2.7.4 HUVEC seeding and culture on discs—Seeding and culture on discs is described in detail in the supplementary material. Briefly, cell suspension was pipetted directly onto each disc and additional growth medium was added around each disc. Cells were incubated at 37 °C and 5% CO_2. Medium was replaced every 24 h. Viability was evaluated at 24, 48, and 72 h via staining with calcein AM and ethidium homodimer-1. For visualization of cell morphology via DAPI staining and indirect immunofluorescence, discs

were removed from the medium after 48 h. Cells were fixed in 4% paraformaldehyde prior to staining and immunocytochemical treatment.

2.7.5 Staining and immunocytochemistry—Staining and immunocytochemistry are described in detail in the supplementary material, and details of reagents are provided in section 2.1. Briefly, following fixation, tube sections or discs were rinsed with 1X PBS and then sequentially treated with permeabilization buffer, blocking buffer, and primary antibody. Samples were then allowed to sit overnight. After removal of the primary antibody, samples were washed with washing buffer, and then treated with secondary antibody. After removal of the secondary antibody, samples were washed with washing buffer and then treated with DAPI in 1X PBS. Following brief incubation with DAPI, samples were washed with washing buffer and imaged via confocal microscopy.

3. Results and discussion

3.1 Coaxial nozzle fabrication

We employed commercially available SLA 3D printers to fabricate coaxial nozzles with intricate, sub-millimeter cross-sectional features and hollow internal geometries. Our basic coaxial nozzle design consisted of a tubular inner conduit supplied by a superior inlet and an annular outer conduit supplied by a lateral inlet (figure 1(b; i) and S6).

The close tolerances of luer lock connectors, as well as the relative brittleness of many cured photopolymer resins, precluded the reliable 3D printing of functional integrated luer lock connectors on the nozzles, using our 3D printers. Therefore, once the nozzles were printed, blunt-tip 14-gauge needles were affixed to the nozzle inlets to provide a means of attachment of syringes via a luer lock connection (figure 1(c; iii, iv)).

In order to provide a large contact area between the printer's build surface and the nozzles, and thus reduce the risk of the nozzles detaching during printing, we included a large superior surface on the nozzles. The nozzles were also designed to be 3D printed without the need for substantial pre-print or post-print processing—e.g. without utilizing support structures. Additionally, strength and rigidity of the nozzles were prioritized in order to resist elastic deformation-induced loss of coaxiality during extrusion and also to resist breakage during use and handling. This consideration entailed, in part, inclusion of thick, tapered walls and placement of the lateral inlet virtually flush with the superior inner surface (i.e. ceiling) of the nozzle (figure S6). Finally, to ensure widespread practicability of this platform, we implemented a modular design; rapid iteration and customization of nozzle models is afforded simply by editing the dimensional constraints of the provided template CAD files (available in the supplementary material). The fully assembled nozzles were used in combination with commercially available pneumatic syringes and adapters for extrusion of shear-thinning hydrogels.

3.2 Fabrication of hydrogel tubes

Shear-thinning hydrogels are ideal for extrusion-based processes (such as 3D printing via direct ink writing (DIW))[40–43] because they readily flow through nozzles during dispensation but then rapidly regain their gel character upon exiting; this enables

maintenance of the extruded form. A material's reversible response to shear load and the time dependence of the response are critical when evaluating a material's suitability for extrusion [44, 45].

In order to ensure fidelity of tubes' cross-sectional profiles to those of the nozzles, we employed two types of hydrogels during the coaxial extrusion process: non-cross-linkable and cross-linkable. A non-cross-linkable hydrogel was formulated from a commercially available amphiphilic triblock copolymer, F127 and was used as a sacrificial core material. A cross-linkable hydrogel was formulated from a derivative of F127, namely, F127-BUM and was employed for the tube walls (figure 1(b)). Irgacure 2959 was added to cross-linkable F127-BUM-based hydrogels as a photo-radical generator.

The F127-BUM was synthesized via reaction of F127 with 2-isocyanatoethyl methacrylate. While there are numerous reports featuring F127 functionalized with (meth)acrylate groups, we found that this particular reaction afforded excellent conversion and facile removal of byproducts. The F127-BUM-based hydrogels retained the rheological characteristics typical of hydrogels of F127 [46, 47]. Namely, the hydrogels exhibited shear-thinning behavior as evidenced by their decreasing apparent viscosities with increasing shear rates, and the rapid recovery of their storage moduli during cyclic shear strain experiments (figures S3–S5).

In addition to their shear-thinning behavior, hydrogels based on F127 or F127-BUM also exhibited a temperature-dependent reversible sol-gel transition, which is driven by a lower critical solution temperature response of the polymer. We have previously reported the utility of the thermo-responsive behavior of these types of hydrogels for the production of shear-thinning nanocomposite materials [48].

The gelation temperatures (T_{gel}) for the F127-BUM-based hydrogels were determined by the cross-over point between the loss and storage moduli in each temperature ramp experiment. For the F127-BUM hydrogel without additive, $T_{gel} \approx 13.7$ °C (figure S3a); for the hydrogel with collagen I additive, $T_{gel} \approx 13.6$ °C (figure S4a); for the hydrogel with AMPS additive, T_{gel} was depressed below 5 °C (figure S5a); however, cooling this gel in an ice bath was sufficient to induce the gel-to-sol transition.

The thermo-responsive behavior of the F127- and F127-BUM-based hydrogels facilitated formulation and processing of these materials. After the gel-to-sol transition was induced for each hydrogel composition, it was possible to transfer these materials into pneumatic syringes without difficulty. The materials were then allowed to return to room temperature, at which point they regained their gel states and were ready for extrusion (figure S7a).

Coaxial filaments comprised of a sacrificial core (29 wt% F127 hydrogel) and a cross-linkable shell (30 wt% F127-BUM hydrogels with or without additives and with photo-radical generator) were extruded using the 3D printed coaxial nozzles. The extruded coaxial filaments were cured with UV light (365 nm) to initiate polymerization of the methacrylate groups and cross-link the outer hydrogel. The coaxial filaments were then rinsed with excess water or PBS to dissolve the uncross-linked sacrificial core hydrogel, yielding a tube.

For purposes of fabricating standalone tubes from F127-BUM-based hydrogels, it is generally not necessary to extrude a sacrificial core hydrogel, but in the event that other hydrogel compositions are utilized, it is likely that an F127-based core hydrogel will be necessary to prevent distortion or collapse of the tube before curing. Furthermore, the core hydrogel was dyed with phenol red to aid in visualization of the lumen size during extrusion, which is convenient if extrusion pressures are not predetermined and are manually adjusted.

In order to demonstrate the versatility of this approach for fabricating tubes of a range of sizes, we employed three different coaxial nozzle sizes. The largest nozzle in this work consisted of an overall orifice diameter (corresponding to the extruded tube outer diameter) of approximately 2 mm (figure S6a); it was used to produce the tubes pictured in figure 2(a; i, ii). The smallest-size nozzle consisted of an overall orifice diameter of approximately 0.5 mm (figure S6c) and was used to produce the smaller tubes pictured in figures 2(a; iii, iv and b). Following fabrication, these small-diameter tubes were submerged in deionized water and perfused with a dye solution to demonstrate patency (figure 2(a; iii, iv)). \When cured, 30 wt% hydrogels based on F127-BUM are relatively tough and elastic. In fact, we were able to tie knots with these tubes (figure 2(a; i)), and also distend them considerably with water (figure S7c).

Luminal diameters and wall thicknesses were determined by the dimensions of the nozzle, as well as the core and shell extrusion pressures. We found that in cases where inner and outer extrusion pressures were well matched, higher fidelity to nozzle dimensions was observed, and overall extrusion rate was adjusted by increasing or decreasing the extrusion pressures in tandem. In cases where the shell extrusion pressure was higher than the core extrusion pressure, the overall extrusion rate (i.e. length of coaxial filament generated per unit time) was limited by the core extrusion rate due to adhesion between the two hydrogels. In these situations, the shell hydrogel exhibited a volumetric flow rate mismatched with the overall extrusion rate, which yielded a tube with a relatively small luminal diameter and a thick wall (figure 2(b); i). In cases where the core extrusion pressure was higher than the shell extrusion pressure, the reverse situation occurred—i.e. a tube with a relatively large luminal diameter and a thin wall was produced (figure 2(b; iii)). In these cases of extrusion-pressure mismatch, overall extrusion rate could still be varied while keeping the coaxial filament geometry approximately constant by adjusting the mismatched pressures in tandem.

The luminal diameters and outer diameters of extruded tubes were found to be generally consistent along the lengths of the tubes. The variations in these dimensions of two different F127-BUM tubes produced using the same (medium-size; 1.25 mm outer conduit diameter) nozzle with different sets of extrusion pressures were evaluated at five different points (approximately 10 mm apart) along the length of each tube (detailed in the supplementary material). For the tube with the smaller lumen, the luminal diameter averaged 0.20 ± 0.01 mm (SD), and the outer diameter averaged 0.74 ± 0.01 mm (SD) (figure S8a; i). For the larger-lumen tube, luminal diameter averaged 0.43 ± 0.01 mm (SD), and the overall diameter averaged 0.70 ± 0.01 mm (SD) (figure S8a; ii).

Extruded tubes or coaxial filaments with more complex cross-sectional profiles may also be fabricated, as seen in figure 2(c). A ‘tube’ with a 5-point star cross-sectional geometry was

generated analogously to other tubes using a coaxial nozzle with a star geometry at its end. This demonstrated that more complex orifice geometries could be modeled at the ends of these nozzles; changing the overall nozzle structure or internal geometry was not necessary.

F127-BUM-based hydrogels can be derivatized with other chemical functionalities via co-polymerization with aqueous-soluble (meth)acrylate monomers. While this approach for introducing chemical species into the hydrogel network has been demonstrated for a range of monomers [45], here we examined the incorporation of 2-acrylamido-2-methyl-1-propanesulfonic acid sodium salt (AMPS) to alter the swelling behavior of the extruded hydrogel tube. A hydrogel formulation with 30 wt% F127-BUM and 10 wt% AMPS was prepared, and its rheological behaviors were evaluated (figure S5). Following fabrication, tubes with and without the AMPS additive were allowed to swell to equilibrium in deionized water. The average water mass fraction of the tubes with AMPS ($n = 4$) was 92.3% ± 0.3% (SD) (figure S8b; i) and the average water mass fraction of the tube without AMPS ($n = 4$) was 82.9% ± 1.3% (SD) (figure S8b; ii).

3.3 Cell seeding experiments

Endothelial cells, which line the luminal surfaces of blood vessels, are one of the principal cellular components of the vascular system, wherein, in addition to fulfilling a variety of other roles, they make up the vascular barrier (endothelium) and control the extravasation of blood proteins and cells. Typical two-dimensional cultures of vascular endothelial cells on glass or poly(styrene) cell cultureware do not recapitulate physiology related to 3D geometry. Consequently, there is considerable interest in widely practicable platforms that enable more representative cultures of vascular endothelial cells [49–51].

Prior to seeding HUVECs on the luminal surfaces of our hydrogel tubes, we first screened our materials for biocompatibility and cell adhesion by producing small (~5 mm in diameter) cross-linked hydrogel discs with identical hydrogel compositions and analogous preparation to our tubes. In preliminary experiments in which we seeded HUVECs on the surfaces of discs made from cross-linked F127-BUM hydrogel without additive, we stained the cells with calcein AM after 24 h in culture in order to visualize cell morphology and infer cell adhesion to the hydrogel surface. These initial results suggested that this material does not promote adhesion of HUVECs—i.e. when cells were seeded directly onto the surfaces of the hydrogel discs, cells retained a rounded morphology as a consequence of a lack of adhesion (figure 3(a; i)). These results were consistent with previous reports [52]. The high poly(ethylene oxide) (PEO) content of F127 (~72%–75%) affords a cross-linked material that resists protein adsorption and cell adhesion [53–57]. It is also worth noting that hydrogels based on F127 or its derivatives are generally not cytocompatible prior to cross-linking, and so these materials are of limited use when cells are to be encapsulated within the material [58].

Thus, collagen I was used to promote cell adhesion to the F127-BUM surface. The thermo-responsive gelation behavior of F127-BUM facilitated the homogenous incorporation of soluble collagen into the hydrogel at low temperatures. Bulk concentrations of collagen I well in excess of 0.2 wt% in the F127-BUM (30 wt%) hydrogels led to substantial aggregation of collagen, causing visible inhomogeneity in the gel, which was detrimental to

extrusion quality. The inclusion of collagen I as an additive at no more than 0.2 wt%, however, was not substantially detrimental to the desirable rheological characteristics of the hydrogel (figure S4) and afforded high-quality tubes.

The adhesion of HUVECs to the hydrogel surface improved substantially with the incorporation of collagen into the hydrogel formulation; however, we observed that the functionalization of F127-BUM hydrogel with collagen I was more effective in promoting HUVEC adhesion when collagen was not only incorporated into the hydrogel formulation prior to fabrication of discs or tubes but also coated onto the cross-linked hydrogel surfaces post-fabrication. The latter was achieved via multiple rounds of rehydration of dehydrated hydrogel constructs (i.e. tubes and discs) in solutions of collagen I. After this process was established, HUVEC morphology and viability were again evaluated by fabricating hydrogel discs functionalized in this way and seeding the cells onto their surfaces. At 24 h in culture, we observed that cells had adhered to the disc surfaces, as evidenced by the spread morphology (figure 3(a; ii)). Beyond cell adhesion, viability of cells cultured on collagen-treated discs made from the F127-BUM hydrogel with collagen I additive was found to be satisfactory after 72 h in culture (figure 3(a; iii)).

Finally, to demonstrate the application of this platform toward the fabrication of models of vascular endothelium, we prepared tubes for the luminal-seeding and culture of HUVECs. Tubes were prepared with the F127-BUM hydrogel with collagen I additive and were treated with collagen I in a manner analogous to the discs discussed above (dehydration/rehydration). To characterize morphology of the HUVECs on the luminal surfaces of tubes, we visualized the interendothelial junction marker CD31 (also referred to as platelet endothelial cell adhesion molecule, PECAM-1) via indirect immunofluorescence after 72 h of culture. The expression and localization of CD31 indicates appropriate general endothelial phenotype [59]. Figures 3(b) and (c) show the presence of interendothelial junctions between HUVECs seeded on the luminal surfaces of collagen-functionalized tubes. Cells were found to exhibit characteristic endothelial cobblestone morphology. Figure 3(b) provides ‘top-down’ views of lumens in the XY plane, showing the coverage of the lumens with HUVECs expressing CD31. Figure 3(c) shows re-constructed z-stacks of a tube lumen that has been seeded with HUVECs. Taken together, these results demonstrate that our coaxial extrusion platform comprised of the coaxial nozzle and F127-BUM-based hydrogels is effective in fabricating collagen-functionalized tubes, and these tubes are suitable for the culture of tubular monolayers of contiguous endothelial cells.

4. Conclusion

In summary, we report a platform for the extrusion-based fabrication of tubular hydrogel constructs using customized, 3D printed coaxial nozzles. These nozzles can be fabricated using commercially available desktop SLA 3D printers and are amenable to use with existing DIW setups. We demonstrate that hydrogels based on a methacrylated Pluronic® F-127 derivative can be extruded through these nozzles to yield multi-material coaxial filaments and tubes with geometries which are tunable either via alteration of nozzle orifice geometry or extrusion pressures. For example, we were able to fabricate tubes with luminal diameters or wall thicknesses as small as ~150 μm, as well as tubes with star-shaped cross-

sectional geometries. Additionally, we demonstrate that tubes produced using our method can be used for 3D culture of HUVECs; this is enabled by functionalization of the F127 derivative hydrogel using collagen I. Our approach ultimately enables the facile fabrication of biofunctional hydrogel conduits which may be useful for engineering *in vitro* models of tubular biological structures.

Supplementary Material

Refer to Web version on PubMed Central for supplementary material.

Acknowledgments

SCM and AN gratefully acknowledge UW Royalty Research Fund for support of this research; AMD and ABT acknowledge funding from the National Institutes of Health (1R35GM128648-01). We thank Dr Abhijit Saha for continued advice and support throughout this work, Ms Xiaojing Su for cell culture support, Mr Ryan Shafranek for synthetic support, and Dr Mark Ganter and Mr Tom Lipton for productive conversations regarding 3D printing and general fabrication.

References

[1]. Monahan-Earley R, Dvorak AM and Aird WC 2013 Evolutionary origins of the blood vascular system and endothelium J. Thromb. Haemostasis 11 46–66 Crossref Google Scholar [PubMed: 23809110]

[2]. Lucas WJ et al. 2013 The plant vascular system: evolution, development and functions J. Integr. Plant Biol. 55 294–388 Crossref Google Scholar [PubMed: 23462277]

[3]. Kolesky DB, Homan KA, Skylar-Scott MA and Lewis JA 2016 Three-dimensional bioprinting of thick vascularized tissues Proc. Natl Acad. Sci. 113 3179–84 Crossref Google Scholar [PubMed: 26951646]

[4]. Homan KA, Kolesky DB, Skylar-Scott MA, Herrmann J, Obuobi H, Moisan A and Lewis JA 2016 Bioprinting of 3D convoluted renal proximal tubules on perfusable chips Sci. Rep. 6 34845 Crossref Google Scholar [PubMed: 27725720]

[5]. Kolesky DB, Truby RL, Gladman AS, Busbee TA, Homan KA and Lewis JA 2014 3D Bioprinting of vascularized, heterogeneous cell-laden tissue constructs Adv. Mater. 26 3124–30 Crossref Google Scholar [PubMed: 24550124]

[6]. Wu W, Deconinck A and Lewis JA 2011 Omnidirectional printing of 3D microvascular networks Adv. Mater. 23 H178–83 Crossref Google Scholar

[7]. O'Bryan CS, Bhattacharjee T, Hart S, Kabb CP, Schulze KD, Chilakala I, Sumerlin BS, Sawyer WG and Angelini TE 2017 Self-assembled micro-organogels for 3D printing silicone structures Sci. Adv. 3 e1602800 Crossref Google Scholar

[8]. Pi Q et al. 2018 Digitally tunable microfluidic bioprinting of multilayered cannular tissues Adv. Mater. 30 1706913 Crossref Google Scholar

[9]. Jia W et al. 2016 Direct 3D bioprinting of perfusable vascular constructs using a blend bioink Biomaterials 106 58–68 Crossref Google Scholar [PubMed: 27552316]

[10]. Ouyang L, Highley CB, Sun W and Burdick JA 2016 A generalizable strategy for the 3D bioprinting of hydrogels from nonviscous photo-crosslinkable inks Adv. Mater. 29 1604983 Crossref Google Scholar

[11]. Song KH, Highley CB, Rouff A and Burdick JA 2018 Complex 3D-printed microchannels within cell-degradable hydrogels Adv. Funct. Mater. 28 1801331 Crossref Google Scholar

[12]. Gao Q, He Y, Fu J-Z, Liu A and Ma L 2015 Coaxial nozzle-assisted 3D bioprinting with built-in microchannels for nutrients delivery Biomaterials 61 203–15 Crossref Google Scholar [PubMed: 26004235]

[13]. Zhang Y, Yu Y, Akkouch A, Dababneh A, Dolati F and Ozbolat I T 2015 In vitro study of directly bioprinted perfusable vasculature conduits Biomater. Sci. 3 134–43 Crossref Google Scholar [PubMed: 25574378]

[14]. Weinberg C and Bell E 1986 A blood vessel model constructed from collagen and cultured vascular cells Science 231 397–400 Crossref Google Scholar [PubMed: 2934816]

[15]. Melchiorri AJ, Bracaglia LG, Kimerer LK, Hibino N and Fisher JP 2016 In vitro endothelialization of biodegradable vascular grafts via endothelial progenitor cell seeding and maturation in a tubular perfusion system bioreactor Tissue Eng. C 22 663–70 Crossref Google Scholar

[16]. Li X, Xu J, Nicolescu CT, Marinelli JT and Tien J 2017 Generation, endothelialization, and microsurgical suture anastomosis of strong 1-mm-diameter collagen tubes Tissue Eng. A 23 335–44 Crossref Google Scholar

[17]. Atlan M, Lellouch AG, Legagneux J, Chaouat M, Masquelet A-C and Letourneur D 2018 A new synthetic model for microvascular anastomosis training? A randomized comparative study between silicone and polyvinyl alcohol gelatin tubes J. Surg. Educ. 75 182 Crossref Google Scholar [PubMed: 28673805]

[18]. Carvalho CR, Costa JB, Morais A DS, López-Cebral R, Silva-Correia J, Reis RL and Oliveira J M 2018 Tunable enzymatically cross-linked silk fibroin tubular conduits for guided tissue regeneration Adv. Healthcare Mater. 71 800186 Crossref Google Scholar

[19]. Syedain ZH, Graham ML, Dunn TB, O'Brien T, Johnson SL, Schumacher RJ and Tranquillo RT 2017 A completely biological 'off-the-shelf' arteriovenous graft that recellularizes in baboons Sci. Transl. Med. 9 eaan4209 Crossref Google Scholar

[20]. Chaouat M, Visage CL, Baille WE, Escoubet B, Chaubet F, Mateescu MA and Letourneur D 2008 A novel cross-linked poly(vinyl alcohol) (PVA) for vascular grafts Adv. Funct. Mater. 18 2855–61 Crossref Google Scholar

[21]. Gao G et al. 2017 Tissue engineered bio-blood-vessels constructed using a tissue-specific bioink and 3D coaxial cell printing technique: a novel therapy for ischemic disease Adv. Funct. Mater. 27 1700798 Crossref Google Scholar

[22]. Duchi S et al. 2017 Handheld co-axial bioprinting: application to in situ surgical cartilage repair Sci. Rep. 7 5837 Crossref Google Scholar [PubMed: 28724980]

[23]. Oberg E, Jones FD, Horton HL, Ryffel HH and McCauley CJ 2016 Machinerys Handbook: A Reference Book For The Mechanical Engineer, Designer, Manufacturing Engineer, Draftsman, Toolmaker and Machinist (New York: Industrial Press) Google Scholar

[24]. Ratcliffe A 2000 Tissue engineering of vascular grafts Matrix Biol. 19 353–7 Crossref Google Scholar [PubMed: 10963996]

[25]. Battiston B, Geuna S, Ferrero M and Tos P 2005 Nerve repair by means of tubulization: literature review and personal clinical experience comparing biological and synthetic conduits for sensory nerve repair Microsurgery 25 258–67 Crossref Google Scholar [PubMed: 15934044]

[26]. Johnson BN et al. 2015 3D printed anatomical nerve regeneration pathways Adv. Funct. Mater. 25 6205–17 Crossref Google Scholar [PubMed: 26924958]

[27]. Atala A, Danilevskiy M, Lyundup A, Glybochko P, Butnaru D, Vinarov A and Yoo JJ 2015 The potential role of tissue-engineered urethral substitution: clinical and preclinical studies J. Tissue Eng. Regen. Med. 11 3–19 Crossref Google Scholar [PubMed: 26631921]

[28]. Raya-Rivera A, Esquiliano DR, Yoo JJ, Lopez-Bayghen E, Soker S and Atala A 2011 Tissue-engineered autologous urethras for patients who need reconstruction: an observational study Lancet 377 1175–82 Crossref Google Scholar [PubMed: 21388673]

[29]. Filippo RED, Yoo JJ and Atala A 2002 Urethral replacement using cell seeded tubularized collagen matrices J. Urol. 168 1789–93 Crossref Google Scholar [PubMed: 12352360]

[30]. Macchiarini P et al. 2008 Clinical transplantation of a tissue-engineered airway Lancet 372 2023–30 Crossref Google Scholar [PubMed: 19022496]

[31]. Yu Y, Zhang Y and Ozbolat IT 2014 A hybrid bioprinting approach for scale-up tissue fabrication J. Eng. Ind. 136 061013 Crossref Google Scholar

[32]. Mistry P, Aied A, Alexander M, Shakesheff K, Bennett A and Yang J 2017 Bioprinting using mechanically robust core–shell cell-laden hydrogel strands Macromol. Biosci. 17 1600472 Crossref Google Scholar

[33]. Colosi C, Shin SR, Manoharan V, Massa S, Costantini M, Barbetta A, Dokmeci MR, Dentini M and Khademhosseini A 2015 Microfluidic bioprinting of heterogeneous 3D tissue constructs using low-viscosity bioink Adv. Mater. 28 677–84 Crossref Google Scholar

[34]. Caliari SR and Burdick JA 2016 A practical guide to hydrogels for cell culture Nat. Methods 13 405–14 Crossref Google Scholar [PubMed: 27123816]

[35]. Hoffman AS 2012 Hydrogels for biomedical applications Adv. Drug Deliv. Rev. 64 18–23 Crossref Google Scholar

[36]. Malda J, Visser J, Melchels FP, Jüngst T, Hennink WE, Dhert WJA, Groll J and Hutmacher DW 2013 25th anniversary article: engineering hydrogels for biofabrication Adv. Mater. 25 5011–28 Crossref Google Scholar [PubMed: 24038336]

[37]. Place ES, Evans ND and Stevens MM 2009 Complexity in biomaterials for tissue engineering Nat. Mater. 8 457–70 Crossref Google Scholar [PubMed: 19458646]

[38]. Obrien FJ 2011 Biomaterials and scaffolds for tissue engineering Mater. Today 14 88–95 Crossref Google Scholar

[39]. Murphy SV and Atala A 2014 3D bioprinting of tissues and organs Nat. Biotechnol. 32 773–85 Crossref Google Scholar

[40]. Liu X, Yuk H, Lin S, Parada GA, Tang T-C, Tham E, Fuente-Nunez CDL, Lu TK and Zhao X 2017 3D Printing of living responsive materials and devices Adv. Mater. 30 1704821 Crossref Google Scholar

[41]. Gioffredi E, Boffito M, Calzone S, Giannitelli SM, Rainer A, Trombetta M, Mozetic P and Chiono V 2016 Pluronic F127 hydrogel characterization and biofabrication in cellularized constructs for tissue engineering applications Proc. CIRP 49 125–32 Crossref Google Scholar

[42]. Suntornnond R, Tan EYS, An J and Chua CK 2017 A highly printable and biocompatible hydrogel composite for direct printing of soft and perfusable vasculature-like structures Sci. Rep. 7 16902 Crossref Google Scholar [PubMed: 29203812]

[43]. Müller M, Becher J, Schnabelrauch M and Zenobi-Wong M 2015 Nanostructured pluronic hydrogels as bioinks for 3D bioprinting Biofabrication 7 035006 IOPscience Google Scholar

[44]. Paxton N, Smolan W, Böck T, Melchels F, Groll J and Jungst T 2017 Proposal to assess printability of bioinks for extrusion-based bioprinting and evaluation of rheological properties governing bioprintability Biofabrication 9 044107 IOPscience Google Scholar

[45]. Smith PT, Basu A, Saha A and Nelson A 2018 Chemical modification and printability of shear-thinning hydrogel inks for direct-write 3D printing Polymer 152 42–50 Crossref Google Scholar

[46]. Prud'homme RK, Wu G and Schneider DK 1996 Structure and rheology studies of poly(oxyethylene−oxypropylene−oxyethylene) aqueous solution Langmuir 12 4651–9 Crossref Google Scholar

[47]. Jalaal M, Cottrell G, Balmforth N and Stoeber B 2017 On the rheology of pluronic F127 aqueous solutions J. Rheol. 61 139–46 Crossref Google Scholar

[48]. Basu A, Saha A, Goodman C, Shafranek RT and Nelson A 2017 Catalytically initiated gel-in-gel printing of composite hydrogels ACS Appl. Mater. Interfaces 9 40898–904 Crossref Google Scholar [PubMed: 29091399]

[49]. Baker BM and Chen CS 2012 Deconstructing the third dimension—how 3D culture microenvironments alter cellular cues J. Cell Sci. 125 3015–24 Crossref Google Scholar [PubMed: 22797912]

[50]. Zheng Y et al. 2012 In vitro microvessels for the study of angiogenesis and thrombosis Proc. Natl Acad. Sci. 109 9342–7 Crossref Google Scholar

[51]. Bischel LL, Sung KE, Jiménez-Torres JA, Mader B, Keely PJ and Beebe DJ 2014 The importance of being a lumen FASEB J. 28 4583–90 Crossref Google Scholar [PubMed: 25077562]

[52]. Fussell GW and Cooper SL 2004 Endothelial cell adhesion on RGD-containing methacrylate terpolymers J. Biomed. Mater. Res. 70A 265–73 Crossref Google Scholar

[53]. Gombotz WR, Guanghui W, Horbett TA and Hoffman AS 1991 Protein adsorption to poly(ethylene oxide) surfaces J. Biomed. Mater. Res. 25 1547–62 Crossref Google Scholar [PubMed: 1839026]

[54]. Harris JM 2014 Poly(ethylene glycol) Chemistry: Biotechnical and Biomedical Applications (New York: Springer Science Business Media, LLC) Google Scholar

[55]. Prime KL and Whitesides GM 1993 Adsorption of proteins onto surfaces containing endattached oligo(ethylene oxide): a model system using self-assembled monolayers J. Am. Chem. Soc. 115 10714–21 Crossref Google Scholar

[56]. Amiji M and Park K 1992 Prevention of protein adsorption and platelet adhesion on surfaces by PEO/PPO/PEO triblock copolymers Biomaterials 13 682–92 Crossref Google Scholar [PubMed: 1420713]

[57]. Wang Y-Q, Wang T, Su Y-L, Peng F-B, Wu H and Jiang Z-Y 2005 Remarkable reduction of irreversible fouling and improvement of the permeation properties of poly(ether sulfone) ultrafiltration membranes by blending with pluronic F127 Langmuir 21 11856–62 Crossref Google Scholar

[58]. Khattak SF, Bhatia SR and Roberts SC 2005 Pluronic F127 as a cell encapsulation material: utilization of membrane-stabilizing agents Tissue Eng. 11 974–83 Crossref Google Scholar [PubMed: 15998236]

[59]. Privratsky JR and Newman PJ 2014 PECAM-1: regulator of endothelial junctional integrity J. Cell Tissue Res. 355 607–19 Crossref Google Scholar

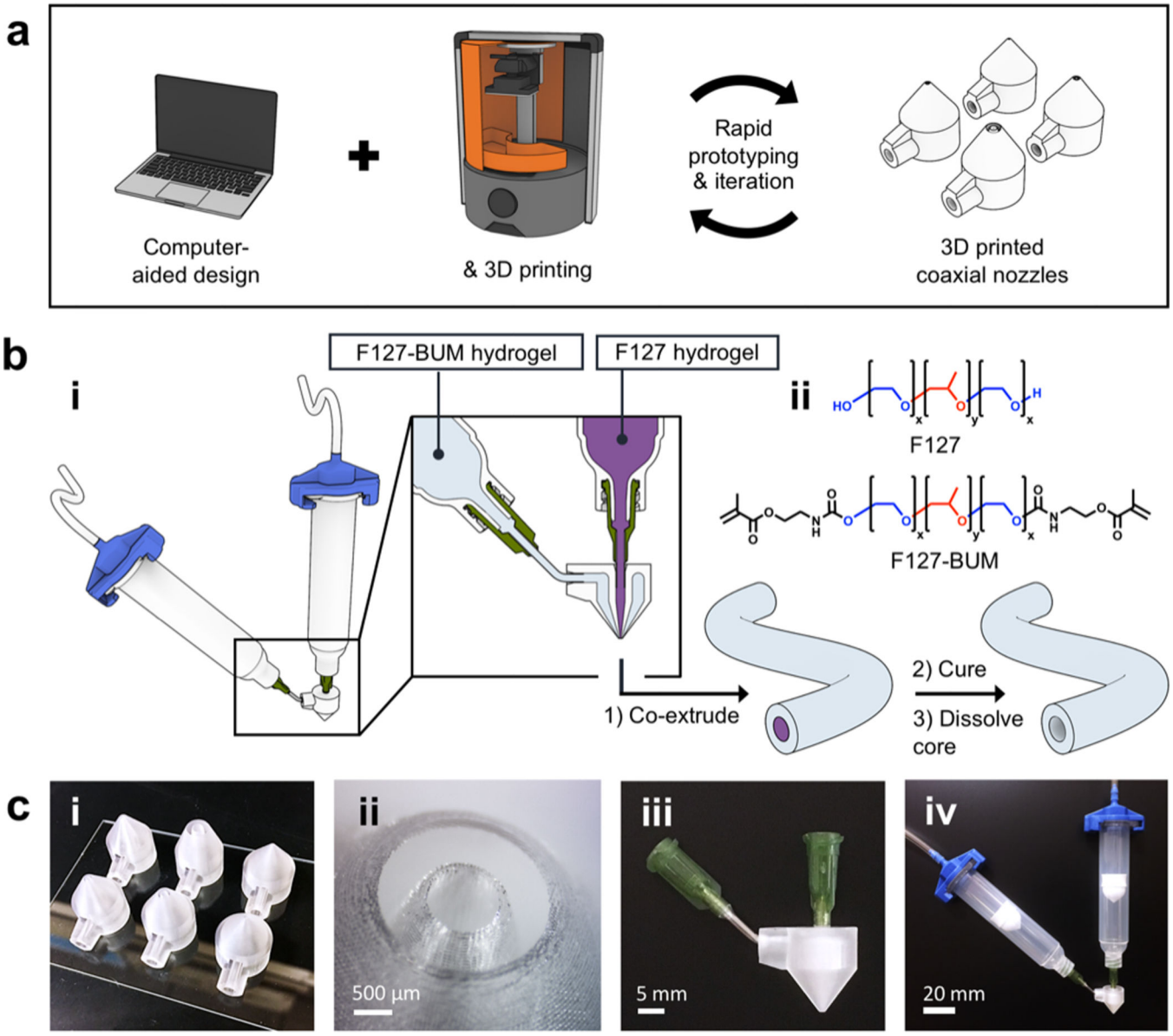

Figure 1.

Schematic of coaxial nozzle and hydrogel tube production. (a) Computer-aided design (CAD) in conjunction with SLA 3D printing enables the fabrication of fully customizable coaxial nozzles. (b; i) Tube fabrication workflow. (b; ii) Chemical structures of F127 and F127-BUM. (c; i) Coaxial nozzles of different diameters after printing. (c; ii) Tip of coaxial nozzle under magnification. (c; iii) Coaxial nozzle after blunt-tip needles have been affixed to inlets. (c; iv) Coaxial extrusion assembly.

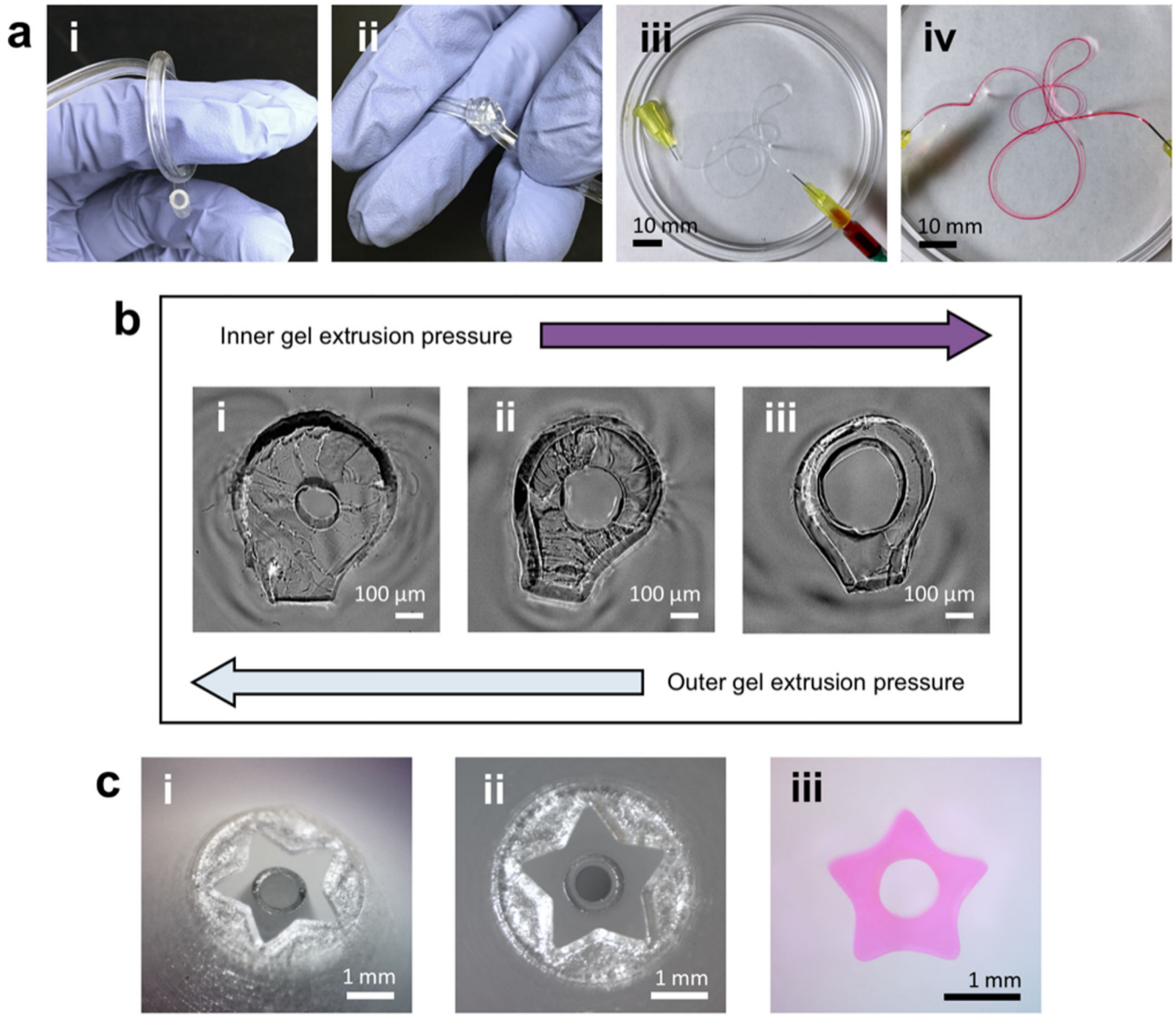

Figure 2.

Tube geometry can be tuned by altering nozzle size and shape as well as extrusion conditions. (a; i, ii) Tubes produced using largest-size (2 mm outer conduit diameter) coaxial nozzle. Tubes have good elasticity and toughness. (a; iii, iv) Tubes fabricated using smallest-size (0.5 mm outer conduit diameter) nozzle. Dye perfusion shows lumen patency. Tube walls were stained as dye began to diffuse through walls. (b) Summary of extrusion-pressure effects on cross-sectional geometry of small tubes. Luminal diameters or wall thicknesses as small as ~150 μm were achieved. (c; i, ii) 5-point star geometry on customized nozzle. (c; iii) Cross-sectional geometry of 5-point star tube produced using star nozzle.

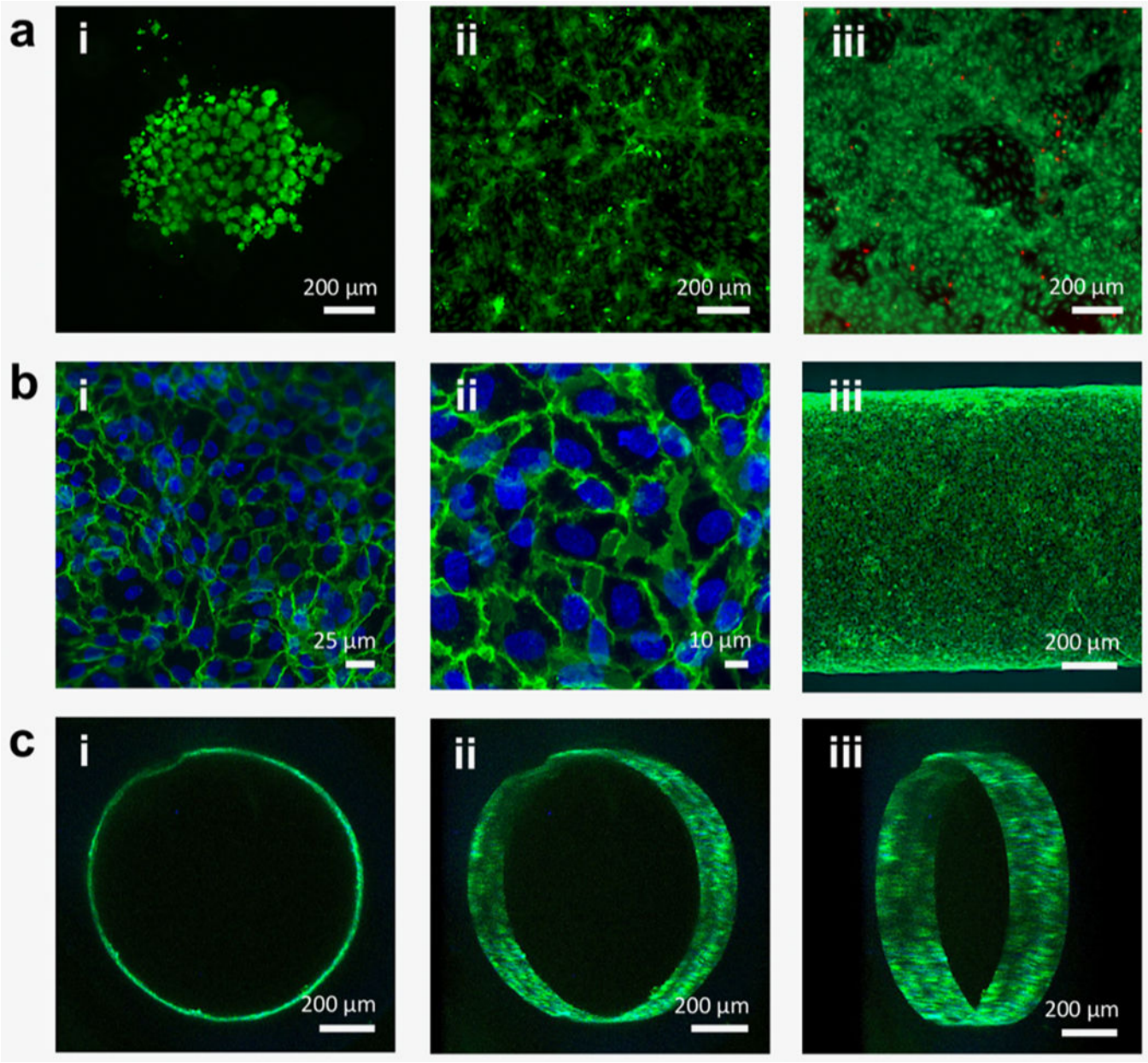

Figure 3.

Fluorescence and confocal micrographs of endothelial cell-seeded, cross-linked hydrogel constructs. (a; i) HUVECs seeded on cross-linked unmodified F127-BUM hydrogel (disc) after 24 h in culture. Cells stained with calcein AM (green) for visualization show aggregation and rounded morphology, indicating lack of adhesion. Percent coverage was determined to be 20% ± 9% (SD; $n = 3$). This image is representative of the three replicates. (a; ii) HUVECs seeded on cross-linked, collagen I-treated F127-BUM hydrogel with collagen I additive (disc) after 24 h in culture. Cells stained with calcein AM for visualization show spreading, indicating adhesion. Percent coverage was determined to be 52% ± 8% (SD; $n = 3$). This image is representative of the three replicates. (a; iii) Viability assay (calcein AM, green/ethidium homodimer-1, red) of HUVECs seeded on cross-linked,

collagen I-treated F127-BUM hydrogel with collagen I additive (disc) after 72 h in culture. Green indicates live cells and red indicates dead cells; cell viability is high. This image is representative of three replicates. (b; i, ii) Confocal micrographs of HUVECs seeded on the luminal surfaces of tubes composed of cross-linked, collagen I-treated F127-BUM hydrogel with collagen I additive. Cells stained with DAPI (blue: nuclei) and labeled via indirect immunofluorescence (green: CD31, interendothelial junction marker) exhibit characteristic cobblestone morphology. These images are representative of six replicates. (b; iii) Identical treatment to (b; i, ii). Entire width of tube section is visualized, showing good cell coverage. This image is representative of six replicates. (c; i, ii, iii) Identical treatment to (b; i, ii, iii). Luminal surface of tube is visualized via confocal microscopy showing good cell coverage. These images are representative of six replicates.